Available online at www.sciencedirect.com
ScienceDirect
Trans. Nonferrous Met. Soc. China 26(2016) 167−174
Transactions of Nonferrous Metals Society of China
www.tnmsc.cn

Erosion-corrosion behavior of Pd−Co and Pd−Cu films on 316L stainless steel in simulated PTA slurry environment

Si-rui LI, Yu ZUO

Beijing Key Laboratory of Electrochemical Process and Technology for Materials, Beijing University of Chemical Technology, Beijing 100029, China

Received 26 February 2015; accepted 24 June 2015

Abstract: Pd−Co films with the Co content varying from 21.9% to 34.62% (mole fraction) and Pd−Cu (5% Cu, mole fraction) film were electrodeposited on 316L stainless steel, and the erosion-corrosion resistance of the Pd−Co and Pd−Cu plated samples in a simulated boiling pure terephthalic acid (PTA) slurry environment was studied with methods of mass loss test, polarization measurement and scanning electron microscopy (SEM). Under the static state condition, both the Pd−Cu and Pd−Co plated samples exhibit good corrosion resistance and the Pd−Cu film behaves slightly better. However, with increasing the stirring speed, the corrosion rate of the Pd−Cu plated samples increases obviously while that of the Pd−Co plated samples shows only slight increase. Higher microhardness and lower surface roughness of Pd−Co film than those of Pd−Cu film, as well as good corrosion resistance, may be the main reasons for better erosion-corrosion resistance in the strong reductive acid plus erosion environment.
Key words: Pd−Co film; Pd−Cu film; 316L stainless steel; electroplating; erosion-corrosion; PTA environment

1 Introduction

Stainless steels show good corrosion resistance in many corrosive media due to their passivity. However, in reductive corrosive media, stainless steels can be severely corroded. One of the examples is that the stainless steel is corroded in the preparation process of pure terephthalic acid (PTA) where acetic acid is used as a solvent at high temperature [1−3]. An effective way to improve the corrosion resistance of stainless steel in reductive corrosive media is surface modification with noble metals such as palladium [4−6]. In our previous studies [7−11], palladium and palladium alloy films were prepared on stainless steels by electroplating and the corrosion resistance was greatly improved in boiling acetic acid and formic acid mixture. However, when pure terephthalic acid (PTA) slurry is involved, the environment is more complicated and the performance of these coatings in such strong erosion-corrosion environment has not been studied.

The degradation of materials due to erosion-corrosion is a major problem in many industries. The synergistic effect of erosion and corrosion can lead to higher degradation rate of materials [12]. The synergism between erosion and corrosion may be illustrated as erosion enhanced corrosion or corrosion enhanced erosion [13]. The former is caused by the retardation in the formation of protective film or even the damage of the protective film on the metal surface. The latter is related to the decrease of surface strength or hardness, and consequently the erosion rate becomes high. In order to obtain an overview of the erosion process, FENG and BALL [14] performed slurry erosion tests on four materials using seven different erodents. The results revealed that for brittle materials, the erosion rate was determined by kinetic energy, particle size, the relative hardness and toughness of erodents. For ductile materials, the shape and kinetic energy of erodents were the most important factors determining the erosion rate while the hardness and toughness of erodents had no significant effect. It was reported that the erosion- corrosion rate depended on the relative hardness of the material [15]. Thus, some researchers have used various surface treatments such as thermal spray coating [16], steered arc deposition [17], double glow process [18] and electroplating [19] to improve the erosion-corrosion properties of materials. SAHA et al [20] prepared

Foundation item: Project (2012BAE04B01) supported by the National Key Technology Research and Development Program of the Ministry of Science and Technology of China
Corresponding author: Yu ZUO; Tel: +86-10-64423795; E-mail: zuoy@mail.buct.edu.cn
DOI: 10.1016/S1003-6326(16)64103-1

microcrystalline and near-nanocrystalline WC−17Co coatings with high velocity oxy-fuel (HVOF) thermal spraying and investigated the erosion-corrosion properties of these two coatings. They concluded that both the coatings owned better erosion-corrosion resistance than the uncoated steel. Furthermore, the near-nanocrystalline coating showed lower erosion-corrosion rate than the microcrystalline coating because the erosion-corrosion mechanism of the former was dominated by corrosion enhanced erosion while that of the latter was dominated by pure erosion.

Previous studies have found that Co was very resistant to erosion-corrosion and cavitation erosion because of its high hardness. Thus, Co-based alloys Stellite 6 and Stellite 21 were developed because of their high cavitation erosion resistance [21]. Some Co-based coatings were also developed and good erosion-corrosion and cavitation resistance were reported [22,23]. Besides, our previous work showed the good corrosion resistance of Pd−Co and Pd−Cu plated 316L stainless steel samples in boiling acetic and formic acid mixture [9,11]. In this work, Pd−Co and Pd−Cu films were electrodeposited on 316L stainless steel, and the erosion-corrosion behavior in a simulated PTA slurry environment was investigated. Current response, potentiodynamic polarization measurements and mass loss tests, combined with scanning electron microscopy (SEM), were used to characterize the erosion-corrosion properties of the Pd–Co and Pd–Cu films in the PTA slurry environment.

2 Experimental

The tested material was 316L stainless steel with the following composition (mass fraction): 16.80% Cr, 13.50% Ni, 0.02% C, 1.40% Mn, 0.32% Si, 0.017% P, 0.014% S, 2.30% Mo and balance Fe.

The samples were cut to the sizes of 20 mm × 10 mm × 2 mm, abraded with abrasive papers up to 1000 grit, then degreased in an alkali solution (30 g/L Na_2CO_3, 30 g/L Na_3PO_4, 50 g/L NaOH) at 70 °C for 30 min, followed by electro-etching in an acidic solution (40 ml/L H_2SO_4, 120 g/L $(NH_4)_2SO_4$) at 40 °C for about 10 min, and rinsed with deionized water. Then, Pd−Co and Pd−Cu alloy films were deposited on 316L stainless steel by electroplating. The solution compositions of Pd−Co and Pd−Cu electroplating are given in Table 1. The applied current density was 10 mA/cm^2, the pH value was in the range of 8−9 and the temperature was kept at 35−45 °C. The electroplating time was 8 min and the thicknesses of both films were 2−3 μm, as shown in Fig. 1.

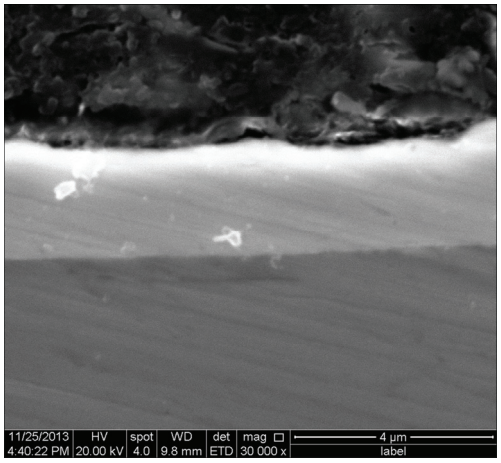

Fig. 1 SEM image of cross section of Pd−Co film

The surface morphologies and compositions of the films were analyzed with a Hitachi S4700 field emission scanning electron microscope (SEM) equipped with an energy dispersive X-ray spectrometer (EDX). The microhardness of the film was measured with a Fischer HM2000 microhardness tester. The load and the dwell time were 20 mN and 20 s, respectively. For each sample, five tests were conducted and the average value was taken. The surface roughness of the films was measured with a Bruker FastScan atomic force microscope (AFM).

The erosion-corrosion tests were performed in boiling 90% acetic acid and 10% formic acid (mass fraction) mixture containing 0.005 mol/L Br^- with the addition of PTA particles with 150 μm in size. The volume ratio of PTA particles to the solution was 1:9. An erosion-corrosion experimental apparatus, consisting of glass cell, high temperature oil-bath, agitator and electrochemical system, was used to investigate the erosion-corrosion behavior of test materials, as shown in Fig. 2. The working electrode was located close to the cell wall, about 50 mm from the cell center. The impact angle of the abrasive solution to the sample was 90° in order to achieve the highest abrasive action. The stirring speeds were 300, 450 and 600 r/min, respectively, to study the effect of the stirring rate. Similar apparatus can be found in Refs. [24,25].

The erosion-corrosion behavior of the deposited films on 316L stainless steel was studied with the methods of electrochemical measurements, mass loss

Table 1 Electroplating solution compositions of Pd−Co and Pd−Cu alloy films (g/L)

Film	$PdCl_2$	NH_4Cl	$NH_3·H_2O$	$(NH_4)_2HPO_4$	EDTA-Cu	EDTA-2NH_4	$CoCl_2·6H_2O$	$C_2H_5O_2N$
Pd−Co alloy	16.6	75	75	0	0	0	16−32	45
Pd−Cu alloy	16.6	75	75	75	2.25	120	0	0

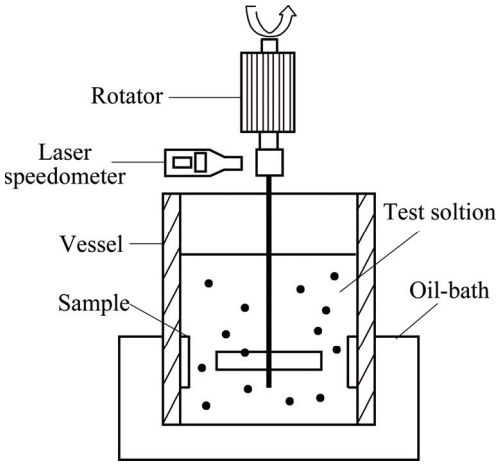

Fig. 2 Schematic diagram of erosion-corrosion test apparatus

tests and microscopic analysis. All the electrochemical measurements including potentiodynamic polarization (PP), current response and open circuit potential (OCP) were carried out using a CS350 electrochemical workstation (Corrtest, Beijing, China). During the electrochemical measurements, the coated steel sample was the working electrode, a saturated calomel electrode (SCE) was the reference electrode, and a platinum plate was the counter electrode. Because the test temperature was relatively high, the SCE was connected to the cell through a long solution bridge so as to maintain the SCE at room temperature. The open circuit potential (OCP) measurement was carried out first under the static condition for about 1800 s, then, the measurement was continued under the erosion-corrosion condition at the stirring speed of 600 r/min. The current response measurements were carried out under static and erosion-corrosion conditions with different stirring speeds at the potential of 450 mV (vs SCE). The scanning rate of potentiodynamic polarization was 0.66 mV/s, and the polarization was started from the potential of 200 mV negative to the open circuit potential. The mass loss tests were carried out in boiling 90% acetic acid and 10% formic acid (mass fraction) mixture with 10% PTA (volume fraction) particles. Different stirring speeds were used and the testing time was 72 h. After the erosion-corrosion tests, the surface morphologies and compositions of samples were observed and analyzed by SEM and EDX analysis, respectively. For the mass loss test and electrochemical tests, three trials were performed in order to ensure the accuracy of the test.

3 Results and discussion

3.1 Characterization of Pd–Co and Pd–Cu films

Figure 3 shows the surface morphologies of the films observed by SEM. Both the Pd−Co and Pd−Cu films show uniform surface without crack and cover the surface well. Table 2 shows the compositions of the Pd−Co and Pd−Cu films determined by EDX and Fig. 4 shows the EDX spectra. The Co content in the Pd−Co films was controlled in a large range from 21.90% to 34.62% (mole fraction), while the Cu content in the Pd−Cu film was set at about 5% (mole fraction) because this film exhibited the best corrosion resistance in boiling 90% acetic acid and 10% formic acid mixture with 0.005 mol/L Br^- [9]. According to the previous XRD analysis [9,11], both the Pd−Cu and Pd−Co alloy films showed single phase FCC structure.

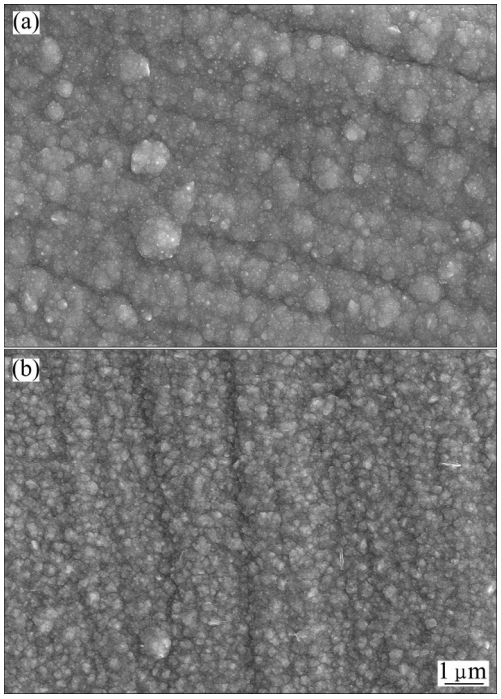

Fig. 3 Surface morphologies of deposited Pd−Co (34.62%Co) (a) and Pd−Cu (b) films

Table 2 EDX results of Pd−Co and Pd−Cu films

Bath composition/ ($g \cdot L^{-1}$)	Mass fraction/%		Mole fraction/%	
	Pd	Co	Pd	Co
16.6 Pd, 16 Co	86.56	13.44	78.10	21.90
16.6 Pd, 24 Co	82.92	17.08	72.90	27.10
16.6 Pd, 32 Co	77.32	22.68	65.38	34.62
16.6 Pd, 2.25 Cu	95.83	3.51	92.24	5.66

Table 3 shows the measured microhardness values of Pd−Co and Pd−Cu films. The Pd−Co films show obviously higher hardness than the Pd−Cu film. With the increase of Co content in the Pd−Co film, the hardness of Pd−Co film increases. The deposited Pd−Co films remain the FCC structure of Pd lattice [11]. The higher hardness of the Pd−Co films may be attributed to the lattice distortion of the Pd−Co solid solution by the

addition of Co. Normally, materials with higher hardness are more resistant to erosion and erosion-corrosion [15,26,27]. Thus, the remarkably high hardness of Pd−Co film would be beneficial to the improvement of the erosion and erosion-corrosion resistance.

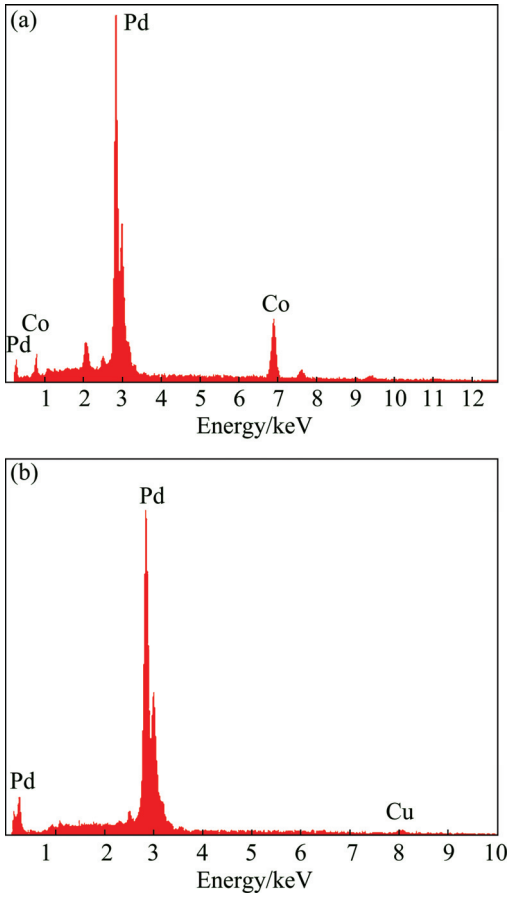

Fig. 4 EDX spectra of Pd−Co (34.62% Co) (a) and Pd−Cu (b) films

Table 3 Microhardness values of Pd−Co and Pd−Cu films (HV)

Pd−Co film (21.9% Co)	Pd−Co film (27.1% Co)	Pd−Co film (34.62% Co)	Pd−Cu film (5.66% Cu)
491.8	548.3	607.1	310.0

The surface roughness of Pd−Cu and Pd−Co films was measured by AFM. Five trials were performed and the profile arithmetic average error, R_a, is the average of these results. For each trial, 10 μm distance was scanned by AFM. For the Pd−Cu film, R_a is 0.076 μm, while for the Pd−Co film, R_a is 0.058 μm. Thus, the surface roughness of Pd−Co film was slightly lower than that of Pd−Cu film.

3.2 Mass loss test

The effect of stirring speed on the erosion-corrosion rate in boiling 90% acetic acid and 10% formic acid mixture containing 0.005 mol/L Br^- with 10% PTA particles was detected by mass loss test, as shown in Fig. 5. The erosion-corrosion rate of the Pd−Co plated samples increases slowly with the increase of stirring speed, whereas that of the Pd−Cu plated samples increases much faster with the increase of stirring speed (from 0 to 600 r/min). The flow velocity is a critical factor influencing the erosion-corrosion process. Many studies [16,28−30] reported that with the increase of flow velocity, the erosion-corrosion rate of test materials increased. Generally, the relationship between the erosion-corrosion rate (w) to flow velocity (v) is expressed as: $w \propto v^n$, where n is a velocity exponent, depending on the actual mechanism of erosion-corrosion, such as the types of materials, impact angle, sand content, particle size [16,31]. In this study, through fitting, the values of n for the Pd−Cu, Pd−Co (21.90% Co), Pd−Co (27.10% Co), and Pd−Co (34.62% Co) plated samples are 1.27, 0.58, 0.36 and 0.30, respectively, which decrease as the film hardness increases. This means that the Pd−Co plated samples are less influenced by the flow velocity than the Pd−Cu plated sample, and with the increase of hardness, the Pd−Co film is more resistant to erosion-corrosion at higher flow velocities.

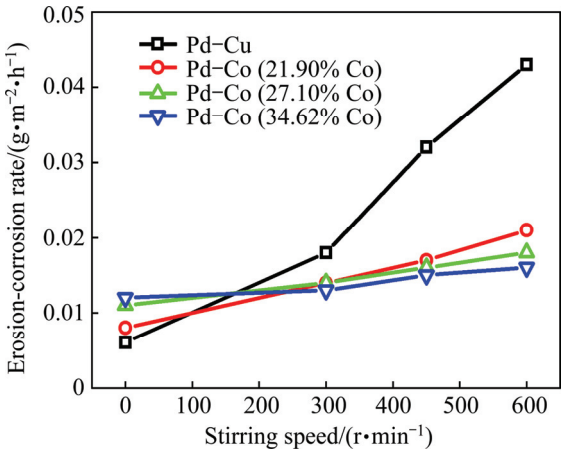

Fig. 5 Variation of erosion-corrosion rate with stirring speed for Pd−Cu and Pd−Co plated samples in boiling PTA slurry environment

3.3 Open circuit potential (OCP) test

To investigate the erosion-corrosion behavior of the Pd−Cu and Pd−Co plated samples in the PTA slurry environment, a series of electrochemical tests were conducted. Firstly, the open circuit potentials of test specimens were measured during the erosion-corrosion process and the results are shown in Fig. 6. The open circuit potentials of all specimens keep stable around 260 mV (vs SCE) under the static state condition, then increase immediately as soon as a stirring speed of 600 r/min was applied. The increase of corrosion potential may be due to that the flow can enhance the transport process of both reactants reaching the metal

surface, which may improve the passivation ability of stainless steels [12,32]. With the extend of test time, the OCP of the Pd−Cu plated sample shows an obvious decrease, suggesting that the corrosion resistance decreases. The OCPs of the Pd−Co plated samples also show slight shift to the negative direction, then keep relatively stable. It is worth noting that the OCP of the Pd−Co (34.62% Co) plated sample is the highest, which suggests that in the tested medium the erosion resistance plays a key role in the erosion-corrosion process. As a result, the Pd−Co (34.62% Co) plated sample that possesses the highest hardness shows the best erosion-corrosion resistance while the Pd−Cu plated sample reveals the lowest erosion-corrosion resistance among the tested samples.

3.4 Current density response test

Figure 7 shows the current density responses of Pd−Cu plated sample and Pd−Co (34.62% Co) plated sample measured in boiling PTA slurry environment at the potential of 450 mV (vs SCE) with different stirring speeds. It is seen that under the static state condition, the recorded current densities for both Pd−Cu and Pd−Co (34.62% Co) plated samples are almost identical, which are close to 18 μA/cm^2. With increasing the stirring speed, the current density of the Pd−Cu plated sample increases rapidly. The increased current density reflects a decrease of corrosion resistance. In comparison, the current density of the Pd−Co (34.62% Co) plated sample increases slowly with increasing the stirring speed. As a result, the current density of the Pd−Co (34.62% Co) plated sample is much lower than that of the Pd−Cu plated sample at higher stirring speed.

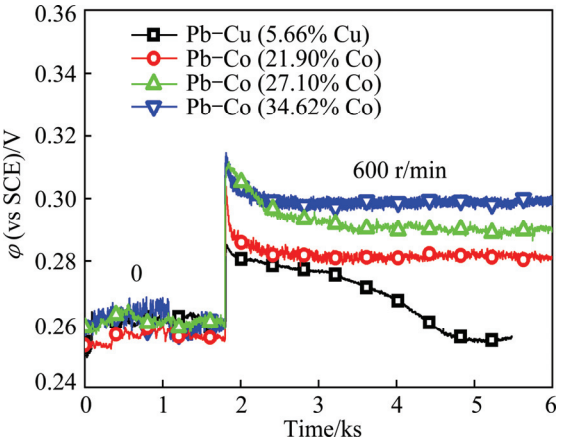

Fig. 6 Open circuit potentials of Pd−Cu and Pd−Co plated samples in boiling PTA slurry environment

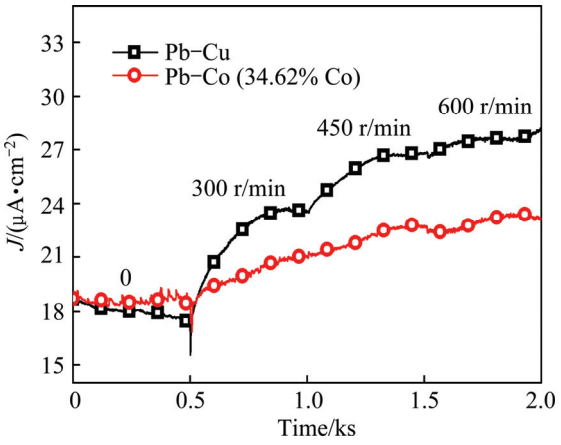

Fig. 7 Current density responses of Pd−Cu and Pd−Co (34.62% Co) plated samples measured at 450 mV (vs SCE) in boiling PTA slurry environment with different stirring speeds of 0, 300, 450 and 600 r/min

3.5 Polarization measurements

Figure 8 presents the polarization curves of Pd−Cu and Pd−Co (34.62% Co) plated samples in boiling PTA slurry environment without stirring or with a stirring speed of 600 r/min after different immersion time. Table 4 shows the electrochemical parameters of the polarization tests. For the Pd−Cu plated sample, after 1 h of immersion, the corrosion potential decreases slightly, and the corrosion current density and anodic current density increase under the slurry flow condition compared with those under the pure corrosion condition. This is in agreement with the open circuit potential test. After 72 h of erosion-corrosion test, the corrosion potential decreases, and the corrosion current density and anodic current density increase further, which suggests that the plated Pd−Cu film may be damaged to some extent. For the Pd−Co (34.62% Co) plated sample, after 1 h of immersion, the corrosion potential increases under the slurry flow condition compared with that under the pure corrosion condition. This may be attributed to that the flow condition can enhance the transport process of the reactants (such as hydrogen ions) reaching the metal surface, which may increase the cathodic reaction rate,

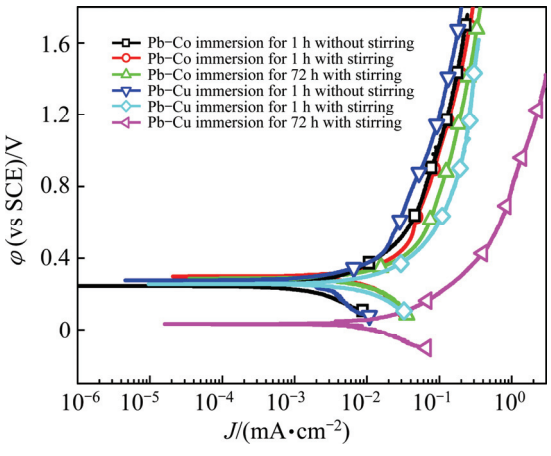

Fig. 8 Polarization curves of samples in boiling PTA slurry environment with different stirring speeds of 0 and 600 r/min and different immersion time

Table 4 Electrochemical parameters for samples in boiling PTA slurry environment with different stirring speeds of 0 and 600 r/min and different immersion time

Condition	J_{corr}/(μA·cm^{-2})	φ_{corr}/mV
Pd−Cu immersion for 1 h without stirring	1.37	276.41
Pd−Cu immersion for 1 h with stirring	3.41	255.43
Pd−Cu immersion for 72 h with stirring	8.14	32.67
Pd−Co immersion for 1 h without stirring	1.45	245.24
Pd−Co immersion for 1 h with stirring	3.08	298.43
Pd−Co immersion for 72 h with stirring	3.53	286.34

leading to increased corrosion potential and corrosion current density. On the other hand, the flow condition can also cause the mechanical damage and induce the decrease of corrosion resistance [12]. The corrosion current density and anodic current density of both the samples increase with the increase of flow velocity, indicating the decrease of corrosion resistance. However, after 72 h of test, the Pd−Co (34.62% Co) plated sample shows obviously lower anodic current density compared with the Pd−Cu plated sample under the slurry flow condition, indicating better erosion-corrosion resistance of Pd−Co plated sample.

3.6 Microscopic analysis after erosion-corrosion test

Figure 9 shows the surface morphologies of the Pd−Cu and Pd−Co (34.62% Co) plated samples after 72 h of erosion-corrosion tests at the stirring speed of 600 r/min. It is evident that large craters are present on the surface of the Pd–Cu plated sample. The elements of stainless steel such as Fe, Cr, Ni and Mo are detected on the exposed area (area 1) and only Pd and Cu are detected on the unexposed surface of the film (area 2) (Figs. 10(a) and (b)). This indicates that the surface of the film is damaged and the substrate is exposed to the solution during the erosion-corrosion test, which will lead to more severe damage. However, for the Pd−Co (34.62% Co) plated sample, the surface looks flat and intact (Fig. 9(b)) and the EDX measurement shows no other element but only Pd and Co on the surface of film (Fig. 10(b)). The results show that the Pd−Co (34.62% Co) plated sample has a better erosion-corrosion resistance than the Pd−Cu plated sample.

Because of good barrier effect and improved passivity, both the Pd−Cu and Pd−Co films can improve the corrosion resistance of 316L stainless steel in boiling acetic acid and formic acid mixture with Br^- [9,11].

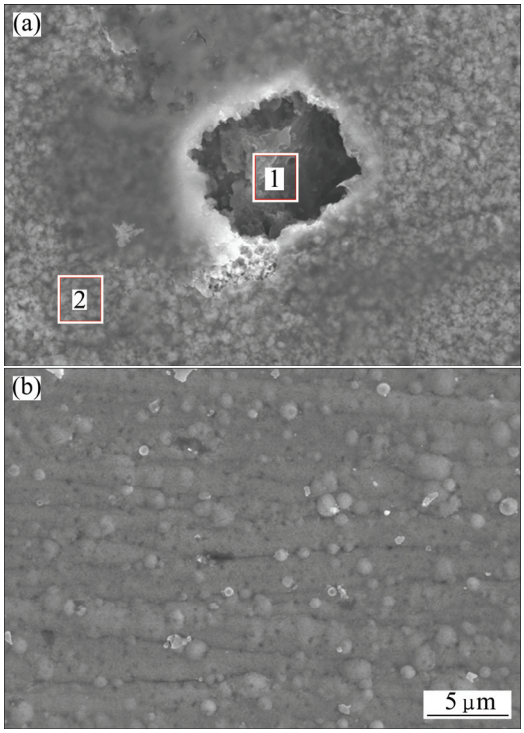

Fig. 9 Surface morphologies of coated samples after 72 h of erosion-corrosion tests at stirring speed of 600 r/min: (a) Pd−Cu plated sample; (b) Pd−Co (34.62% Co) plated sample

However, during the erosion-corrosion process with the PTA particles impacting the surface, the mass loss of all samples increases (Fig. 5). With the increase of stirring speed, the erosion process will be enhanced and combined with the corrosion process, further decreasing the resistance of materials [16,33]. But with the increase of microhardness, the Pd−Co plated samples show better erosion-corrosion resistance, especially for the Pd−Co (34.62% Co) plated sample. As for the Pd−Cu plated sample, the film was damaged by the impact of PTA particles (Figs. 9(a) and 10(a)). Therefore, in the boiling PTA slurry environment, the Pd−Co plated samples show better erosion-corrosion resistance than the Pd−Cu plated sample, and with increasing the hardness of Pd−Co films, the erosion-corrosion resistance also increases. In addition, the surface roughness of the Pd−Co (34.62% Co) film is lower than that of the Pd−Cu film, which also benefits to improving the erosion resistance. It is noted that under the static condition, the Pd−Cu plated samples show slightly better corrosion resistance than the Pd–Co plated samples, while under the stirring condition, the Pd−Co plated samples behave much better. Therefore, although Pd or Pd alloys plated stainless steel samples show quite good corrosion resistance in strong, reductive corrosion media [7−11], the long term performance will depend on the lifetime of the films on the surface. In the

media with erosion, the erosion resistance of the film will become the key factor for long performance. The above results provide a new selection to protect stainless steels in slurry PTA environment.

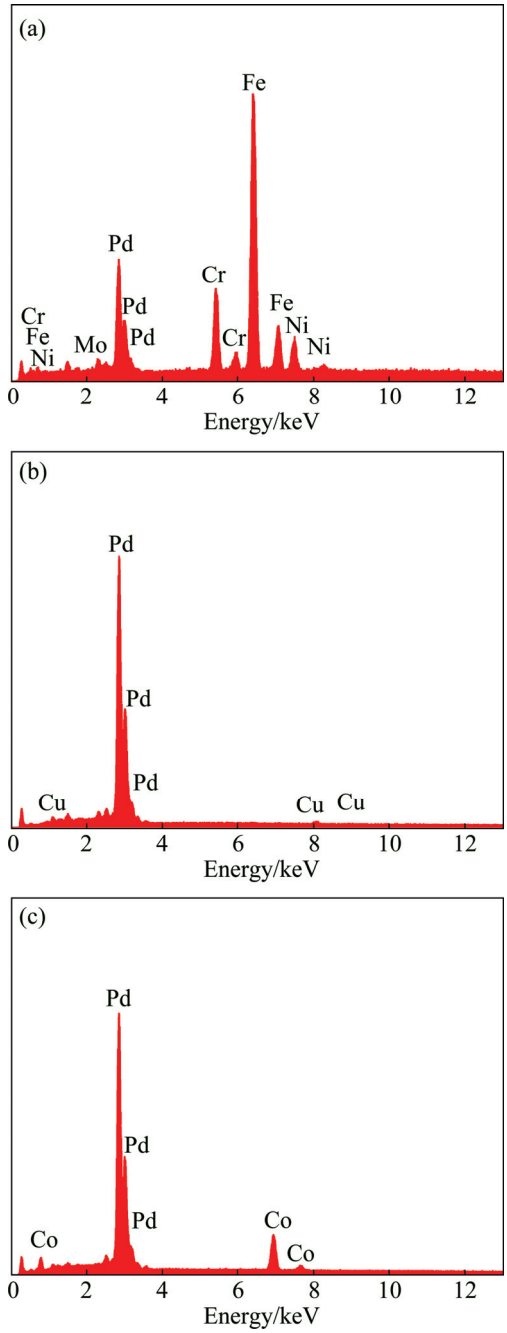

Fig. 10 EDX spectra of area 1 (a) and area 2 (b) in Fig. 9(a) and Pd−Co plated sample in Fig. 9(b) (c)

4 Conclusions

1) Pd−Co films with the Co content varying from 21.9% to 34.62% and Pd−Cu (5% Cu) film were electrodeposited on 316L stainless steel. The microhardness of the Pd−Co film increases with increasing the Co content in the film. The Pd−34.62% Co film shows the highest hardness of HV 607.1, almost twice of that of Pd−5% Cu film.

2) In simulated boiling PTA slurry environment, under static state condition, both the Pd−Cu and Pd−Co plated samples exhibit good corrosion resistance and the Pd−Cu film behaves slightly better. However, with increasing the stirring speed, the corrosion rate of the Pd−Cu plated samples increases obviously while that of the Pd−Co plated samples shows only slight increase.

3) The obviously higher microhardness and lower surface roughness of the Pd−Co film than those of Pd−Cu film, as well as good corrosion resistance, may be the main reasons for better erosion-corrosion resistance of the Pd−Co plated stainless steel samples in the strong reductive acid plus erosion environment.

References

[1] JU P F, ZUO Y, TANG J L, TANG Y M. Corrosion behaviour of 316L stainless steel in PTA slurry [J]. Corrosion Engineering Science and Technology, 2013, 8: 207−210.

[2] SEKINE I, HATAKEYAMA S, NAKAZAWA Y. Corrosion behaviour of type 430 stainless steel in formic and acetic acids [J]. Corrosion Science, 1987, 27(3): 275−288.

[3] SEKINE I, HATAKEYAMA S, NAKAZAWA Y. Effect of water content on the corrosion behaviour of type 430 stainless steel in formic and acetic acids [J]. Electrochimica Acta, 1987, 32: 915−920.

[4] OLUBAMBI P A, POTGIETER J H, CORNISH L. Corrosion behaviour of superferritic stainless steels cathodically modified with minor additions of ruthenium in sulphuric and hydrochloric acids [J]. Materials and Design, 2009, 30(5): 1451−1457.

[5] BROSSIA C S, GRAGNOLINO G A. Effect of palladium on the corrosion behavior of titanium [J]. Corrosion Science, 2004, 46(7): 1693−1711.

[6] SHERIF E M, POTGIETER J H, COMINS J D, CORNISH L, OLUBAMBI P A, MACHIO C N. The beneficial effect of ruthenium additions on the passivation of duplex stainless steel corrosion in sodium chloride solutions [J]. Corrosion Science, 2009, 51(6): 1364−1371.

[7] TANG Jun-lei, ZUO Yu. Study on corrosion resistance of palladium films on 316L stainless steel by electroplating and electroless plating [J]. Corrosion Science, 2008, 50(10): 2873−2878.

[8] XU Liang, ZUO Yu, TANG Jun-lei, TANG Yu-ming, JU Peng-fei. Chromium−palladium films on 316L stainless steel by pulse electrodeposition and their corrosion resistance in hot sulfuric acid solutions [J]. Corrosion Science, 2011, 53(11): 3788−3795.

[9] GAO Xiang, TANG Jun-lei, ZUO Yu, TANG Yu-ming, XIONG Jin-ping. The electroplated palladium−copper alloy film on 316L stainless steel and its corrosion resistance in mixture of acetic and formic acids [J]. Corrosion Science, 2009, 51(8): 1822−1827.

[10] JU Peng-fei, ZUO Yu, TANG Jun-lei, TANG Yu-ming, HAN Zhong-zhi. The characteristics of a Pd–Ni/Pd–Cu double coating on 316L stainless steel and the corrosion resistance in stirred boiling acetic and formic acids mixture [J]. Materials Chemistry and Physics, 2014, 144(3): 263−271.

[11] LI Si-rui, ZUO Yu, TANG Yu-ming, ZHAO Xu-hui. The electroplated Pd–Co alloy film on 316L stainless steel and the corrosion resistance in boiling acetic acid and formic acid mixture with stirring [J]. Applied Surface Science, 2014, 321: 179−187.

[12] ZHENG Yu-gui, YAO Zhi-ming, WEI Xiang-yun, KE Wei. The synergistic effect between erosion and corrosion in acidic slurry medium [J]. Wear, 1995, 186−187: 555−561.

[13] STACK M M, ADB EL BADIA T M. Mapping erosion-corrosion of WC/Co−Cr based composite coatings: Particle velocity and applied potential effects [J]. Surface and Coatings Technology, 2006, 201(3−4): 1335−1347.
[14] FENG Z, BALL A. The erosion of four materials using seven erodents—Towards an understanding [J]. Wear, 1999, 233−235: 674−684.
[15] MOHAMMADI F, LUO J L. Effect of cold work on erosion-corrosion of 304 stainless steel [J]. Corrosion Science, 2011, 53(2): 549−556.
[16] WANG Y, ZHENG Y G, KE W, SUN K H, HOU W L, CHANG X C, WANG J Q. Slurry erosion-corrosion behaviour of high-velocity oxy-fuel (HVOF) sprayed Fe-based amorphous metallic coatings for marine pump in sand-containing NaCl solutions [J]. Corrosion Science, 2011, 53(10): 3177−3185.
[17] TU J P. The effect of TiN coating on erosion-corrosion resistance of α-Ti alloy in saline slurry [J]. Corrosion Science, 2000, 42(1): 147−163.
[18] XU Jiang, ZHUO Cheng-zhi, HAN De-zhong, TAO Jie, LIU Lin-lin, JIANG Shu-yun. Erosion-corrosion behavior of nano-particle-reinforced Ni matrix composite alloying layer by duplex surface treatment in aqueous slurry environment [J]. Corrosion Science, 2009, 51(5): 1055−1068.
[19] JUNEGHANI M A, FARZAM M, ZOHDIRAD H. Wear and corrosion resistance and electroplating characteristics of electrodeposited Cr−SiC nano-composite coatings [J]. Transactions of Nonferrous Metals Society of China, 2013, 23(7): 1993−2001.
[20] SAHA G C, KHAN T I, ZHANG G A. Erosion-corrosion resistance of microcrystalline and near-nanocrystalline WC−17Co high velocity oxy-fuel thermal spray coatings [J]. Corrosion Science, 2011, 53(6): 2106−2114.
[21] ROMO S A, SANTA J F, GIRALDO J E, TORO A. Cavitation and high-velocity slurry erosion resistance of welded Stellite 6 alloy [J]. Tribology International, 2012, 47: 16−24.
[22] SANTA J F, BLANCO J A, GIRALDO J E, TORO A. Cavitation erosion of martensitic and austenitic stainless steel welded coatings [J]. Wear, 2011, 271(9−10): 1445−1453.
[23] DING Zhang-xiong, CHEN Wei, WANG Qun. Resistance of cavitation erosion of multimodal WC−12Co coatings sprayed by HVOF [J]. Transactions of Nonferrous Metals Society of China, 2011, 21(10): 2231−2236.
[24] CALDERÓN J A, HENAO J E, GÓMEZ M A. Erosion-corrosion resistance of Ni composite coatings with embedded SiC nanoparticles [J]. Electrochimica Acta, 2014, 124: 190−198.
[25] LI J L, MA H X, ZHU S D, QU C T, YIN Z F. Erosion resistance of CO_2 corrosion scales formed on API P110 carbon steel [J]. Corrosion Science, 2014, 86: 101−107.
[26] CHACON NAVA J G, STOTT F H, STACK M M. The effect of substrate hardness on the erosion-corrosion resistance of materials in low-velocity conditions [J]. Corrosion Science, 1993, 35(5−8): 1045−1051.
[27] NEVILLE A, HODGKIESS T, DALLAS J T. A study of the erosion-corrosion behaviour of engineering steels for marine pumping applications [J]. Wear, 1995, 186−187: 497−507.
[28] MAHDI E, RAUF A, ELTAI E O. Effect of temperature and erosion on pitting corrosion of X100 steel in aqueous silica slurries containing bicarbonate and chloride content [J]. Corrosion Science, 2014, 83: 48−58.
[29] PURANDARE Y P, STACK M M, HOVSEPIAN P Eh. Velocity effects on erosion-corrosion of CrN/NbN “superlattice” PVD coatings [J]. Surface and Coatings Technology, 2006, 201(1−2): 361−370.
[30] STACK M M, CHACON-NAVA J, STOTT F H. Relationship between the effects of velocity and alloy corrosion resistance in erosion-corrosion environments at elevated temperatures [J]. Wear, 1995, 180(1−2): 91−99.
[31] BJORDAL M, BARDAL E, ROGNE T, EGGEN T G. Erosion and corrosion properties of WC coatings and duplex stainless steel in sand-containing synthetic sea water [J]. Wear, 1995, 186−187: 508−514.
[32] SASAKI K, BURSTEIN G T. Erosion-corrosion of stainless steel under impingement by a fluid jet [J]. Corrosion Science, 2007, 49(1): 92−102.
[33] LÓPEZ D, CONGOTE J P, CANO J R, TORO A, TSCHIPTSCHIN A P. Effect of particle velocity and impact angle on the corrosion-erosion of AISI 304 and AISI 420 stainless steels [J]. Wear, 2005, 259(1−6): 118−124.

316L 不锈钢表面 Pd−Co 膜层和 Pd−Cu 膜层在模拟 PTA 环境中的冲刷腐蚀性能

李思锐，左 禹

北京化工大学 材料电化学过程与技术北京市重点实验室，北京 100029

摘 要：用电沉积方法在 316L 不锈钢表面制备 Co 含量为 21.9%~34.62%(摩尔分数)的 Pd−Co 膜层和 Cu 含量为 5%(摩尔分数)的 Pd−Cu 膜层，通过失重试验、极化曲线以及扫描电子显微镜等方法研究镀膜不锈钢试样在模拟纯对苯二甲酸(PTA)冲刷腐蚀环境中的耐冲刷腐蚀性能。结果表明：在静止环境中，Pd−Cu 及 Pd−Co 膜层试样都表现出良好的耐蚀性，且 Pd−Cu 膜层试样的耐蚀性更优。但是，随着搅拌速度的增大，Pd−Cu 膜层试样的冲刷腐蚀速率大大增加，而 Pd−Co 膜层试样的冲刷腐蚀速率仅有微小增加。与 Pd−Cu 镀层相比，Pd−Co 镀层在所研究介质中的耐腐蚀性大致相当，但具有更高的硬度和更小的表面粗糙度，从而在具有冲刷环境的强还原性酸性介质中显示出优异的抗冲刷腐蚀性能。

关键词：Pd−Co 膜；Pb−Cu 膜；316L 不锈钢；电镀；冲刷腐蚀；PTA 环境

(Edited by Mu-lan QIN)